RSC Advances

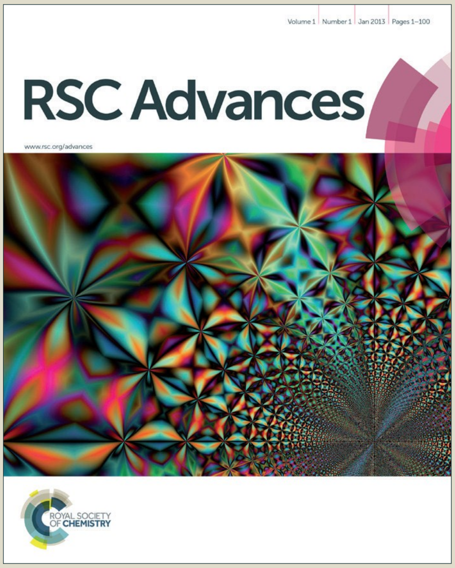

ROYAL SOCIETY OF CHEMISTRY

www.rsc.org/advances

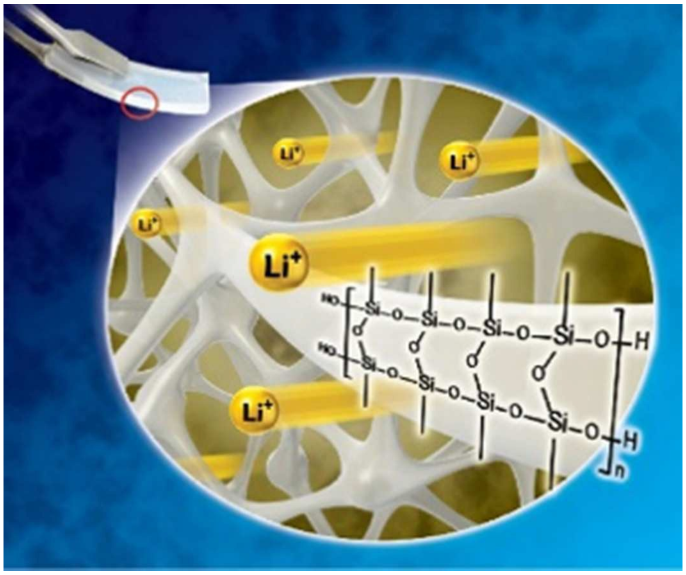

162x135mm (53 x 53 DPI)

Journal Name

ARTICLE

# Ion Conduction Behaviour in Chemically Crosslinked Hybrid Ionogels: Effect of Free-dangling Oligoethyleneoxides

Received 00th January 20xx,
Accepted 00th January 20xx

DOI: 10.1039/x0xx00000x

**www.rsc.org/**

Albert S. Lee,[a†] Jin Hong Lee,[a,b†] Soon Man Hong,[a,c] Jong-Chan Lee,[b] Seung Sang Hwang[a,c]* and Chong Min Koo[a,c]*

A series of PEO-functionalized, ladder-like structured polysilsesquioxane copolymers were synthesized and utilized for the fabrication of PEGylated hybrid ionogels through chemical crosslinking of the ionic liquid, 1M LiTFSI in N-butyl-N-methylpyrrolidinium bis(trifluoromethylsulfonyl)imide. Through a systematic variance of the copolymer concentration of methacryloxypropyl- and PEG groups, we were able to demonstrate enhanced ionic conductivity and lithium ion dissociation as the PEO content increased. Through an in-depth spectroscopic investigation of the ion conduction behavior of these PEGylated hybrid ionogels and comparison with hybrid ionogels without PEG groups, we were able to demonstrate how enhancement in lithium ion battery performance for PEGylated hybrid iongels could be achieved at identical crosslinker concentrations.

## Introduction

With the ever increasing demand for next generation electrochemical cells to achieve higher performance, often overlooked are the safety issues arising from the thermal and mechanical stability of organic liquid electrolytes.[1,2] And with the applications requiring high performance electrochemical cells: electronic devices such as portable laptops, cell phones, and hybrid/fully electronic vehicles all being utilized in close range by humans, safety concerns over electrolyte leakage and thermal expansion have been well-documented.[3,4] Further exacerbating this issue is the flammability of electrolyte solutions, which are comprised of lithium salts dissolved in highly flammable carbonate-based organic solvents.[5,6]

In order to alleviate the above safety concerns, ionogels have recently garnered great interest in the academic community. Ionogels are defined as ion conducting liquids solidified through physical or chemical crosslinks, usually through the use of crosslinkable polymeric gelators.[7-9] Through tuning of both the content and composition of the solidifying gelator, various ionogels have been fabricated, and their utility for practical electrochemical performance confirmed.[10-12] However, even these ionogels crosslinked with organic gelator materials lacked the necessary thermal and mechanical properties, leading to excess use of crosslinking material, invariably depreciating ion mobility and electrochemical performance.[13,14]

The hybridization of the crosslinking matrix network to attain hybrid ionogels has also been a booming field of interest to alleviate the above concerns of low thermal, mechanical, and ion transport properties. The gelation of ionic conducting solutions with various inorganic-organic hybrid materials such as ORMOCERs,[15] inorganic oxides,[16-18] and polysilsesquioxanes[10] have been extensively investigated. However, many of these approaches have entailed the use of organic moiety for only crosslinking function. Additionally, inorganic-oxides, such as nano-sized silica and alumina, have shown great promise due to their ability to gel ionic conducting solutions through the aggregation of inorganic networks, following the Derjaguin-Landau-Verwey-Overbeek (DLVO) theory.[19] Pioneering works by the Archer group[11,12,20,21] have investigated hybrid ionogels gelled through silane surface-modified metal oxides. Through surface modification of ionic liquid groups, oligo-ethylene oxide groups, and single ion conducting groups, all functioning to improve the electrical properties of the hybrid ionogels, these hybrid ionogels have been pioneering in improving the thermal stability, mechanical properties and ion mobility. However, these hybrid ionogels still suffer from the fact that they can only be dispersed, not homogenously dissolved in ion conducting solutions,[18,22] and that the degree of control over mechanical properties is low compared with chemically crosslinked hybrid ionogels.

In our previous study, we investigated hybrid gel polymer electrolytes and hybrid ionogels fabricated with a methacryloxypropyl-functionalized ladder-structured polysilsesquioxane homopolymer. Ladder-structured polysilsesquioxanes,[10, 23] which are comprised of an inorganic Si-O-Si ladder backbone, with radial organic functional groups,

---

[a] *Materials Architecturing Research Centre, Korea Institute of Science and Technology, Hwarangno 14-gil 5, Seong-Buk Gu, Seoul 136-791.*
[b] *Department of Chemical and Biological Engineering, and Institute of Chemical Process, Seoul National University, 599 Gwanak-ro, Gwanak-gu, Seoul 151-744.*
[c] *Nanomaterials Science and Engineering, University of Science and Technology, 217 Gajungro, 176 Gajung-dong, Yuseong-Gu, Daejeon, Korea 305-333*

† *These authors contributed equally.*

*Electronic Supplementary Information (ESI) available: [FTIR spectra, picture of vial, structure of LPMASQ, LSV, TGA, charge-discharge profiles with BMPTFIS celss ]. See DOI: 10.1039/x0xx00000x* exhibited high solubility in various ion conducting solutions, and thus we were able to tune the mechanical properties such that liquid-like ionic conductivity was able to be attained without sacrificing gel robustness.

In this study, we sought out to investigate the effect of free-dangling oligomeric polyethyleneoxide groups copolymerized with methacryloxypropyl- groups at various comonomer ratios on the ion conduction behavior of chemically crosslinked hybrid ionogels. We stipulated that through introduction of the free-dangling oligomeric polyethyleneoxide groups into the inorganic ladder-structured backbone at the molecular level, the inorganic backbone would function as support for mechanical robustness, while the PEO groups would contribute to enhanced ion conduction behavior through an in-depth spectroscopic analysis of these PEGylated hybrid ionogels compared to our previously studied hybrid ionogels.

## Experimental

### Materials

2-[methoxy(polyethyleneoxy)propyl]trimethoxysilane (Gelest, 90%), 3-methacryloxypropyltrimethoxysilane (Shin-Etsu, 98%), and ethyl acetate (J.T. Baker, HPLC grade) were distilled over $CaH_2$ prior to use. Potassium carbonate (Daejung) was dried at 40 °C. THF (J.T. Baker, HPLC grade) was distilled over sodium. Azobisisobutyronitrile (Daejung Chemicals, 99%) was recrystallized from methanol. Lithium bis(trifluoromethylsulfonyl)imide (LiTFSI) (Aldrich, 99.9%, battery grade) and N-butyl-N-methylpyrrolidinium bis(trifluoromethylsulfonyl)imide (BMPTFSI) (C-TRI, 99.9%) were used dried in a vacuum oven and stored in a argon-charged glove box prior to use.

### Synthesis of LPEOMASQ series

LPEOMASQ was synthesized following a modified literature procedure.[24, 25] In a typical experiment, potassium carbonate, $K_2CO_3$ (0.04 g, 0.29 mmol) was dissolved in deionized $H_2O$ (4.8 ml, 0.27 mol) and 8 g of THF was added. To this solution, 3-methacryloxypropyltrimethoxysilane (9.9 ml, 0.04 mol) and 2-[methoxy(polyethyleneoxy)propyl]trimethoxysilane (19 ml, 0.04 mol) were added dropwise under nitrogen flow. The solution was magnetically stirred for 10 days when the molecular weight reached its maximum value. After partial evaporation of THF, the resinous material was dissolved in dichloromethane and extracted several times with water. Collection of the organic layers followed by drying of the organic layer over anhydrous magnesium sulphate and evaporation of the solvent under reduced pressure yielded a transparent liquid with medium viscosity (22 g, 92% crude yield). LPEOMASQ was found to have excellent solubility in the majority of organic solvents of medium to high polarity. LPEOMASQs with 3 different methacryloxypropyl:polyethyleneoxide mol ratios, 25:75, 50:50, 75:25, were synthesized by simply varying the initial feed comonomer ratio and the samples were named LPEOMASQ25, LPEOMASQ50, and LPEOMASQ75, accordingly to the PEO-copolymer composition percentage.

$^1$H NMR ($CDCl_3$) (δ, ppm):
0.35-0.45 (m, $\mathrm{Si(C\mathit{H}_2CH_2CH_2OCOCCH_2CH_3}$, $\mathrm{SiC\mathit{H}_2CH_2CH_2O(CH_2CH_2O)_{6\text{-}9}CH_3}$, 4H),
1.8-1.9 (m, $\mathrm{Si(CH_2C\mathit{H}_2CH_2OCOCCH_2CH_3}$, $\mathrm{SiCH_2C\mathit{H}_2CH_2O(CH_2CH_2O)_{6\text{-}9}CH_3}$, 4H),
1.95-2.05 (m, $\mathrm{Si(CH_2CH_2CH_2OCOCCH_2C\mathit{H}_3}$, 3H),
3.15-3.3 (m, $\mathrm{Si(CH_2CH_2C\mathit{H}_2OCOCCH_2CH_3}$, $\mathrm{SiCH_2CH_2C\mathit{H}_2O(CH_2CH_2O)_{6\text{-}9}CH_3}$, 4H),
3.7-3.8 (m, $\mathrm{SiCH_2CH_2CH_2O(C\mathit{H}_2C\mathit{H}_2O)_{6\text{-}9}CH_3}$, 30H),
4.08-4.16 (m, $\mathrm{SiCH_2CH_2CH_2O(CH_2CH_2O)_{6\text{-}9}C\mathit{H}_3}$, 3H),
5.3-6.1 (m, $\mathrm{Si(CH_2CH_2CH_2OCOCC\mathit{H}_2CH_3}$, 2H)
$^{29}$Si NMR (ppm): -68~-70 ppm,
$M_w$ = 24.3 k.

### Characterization and Measurements

Fourier transform infrared spectra were measured with a Perkin-Elmer FT-IR system Spectrum-GX on cast KBr plates. Raman spectra were obtained with a Renishaw InVia spectrometer equipped with 633 nm HeNe laser. Weight averaged molecular weight ($M_w$) and molecular weight distributions ($M_w/M_n$) of polymers were measured using JASCO PU-2080 plus SEC system equipped with refractive index detector (RI-2031 plus), UV detector (λ = 254 nm, UV-2075 plus) and Viscotek SLS apparatus using THF as the mobile phase at 40 °C with a flow rate of 1 mL min$^{-1}$. The samples were separated through four columns (Shodex-GPC KF-802, KF-803, KF-804, KF-805). Solution-state $^1$H-NMR and $^{29}$Si NMR spectra were recorded in $CDCl_3$ at 25 °C using a Varian Unity INOVA ($^1$H: 300 MHz, $^{29}$Si: 59.6 MHz). Solid-state $^7$Li NMR and $^{19}$F NMR spectra were obtained on a Varian INOVA ($^1$H: 400 MHz, $^7$Li: 155.45 MHz, $^{19}$F: 376.3 MHz), with spinning frequency held constant at 10 kHz with a pulse delay time of 4 s. Samples were packed into 7.5 mm zirconia rotors and sealed with Kel-F short caps. Thermal gravimetric analysis was carried out with TA instrument (TGA 2950) at heating rate of 10 °C min$^{-1}$ under $N_2$ atmosphere. Rheological properties were examined using a rheometer (Advanced Rheometric Expansion System, ARES) instrument with cone-plate geometry (25 mm diameter). All rheological measurements were performed in the linear viscoelastic region under $N_2$ atmosphere. The ionic conductivity was determined using a complex impedance analyzer (Bio-Logics, VMP3) over frequency range from 1 Hz to 1 MHz at AC amplitude of 10 mV. The electrochemical stability of the gel polymer electrolytes was examined using a linear sweep voltammetry system. In the experiments, a stainless steel working electrode was used with lithium metal as both the counter and reference electrodes. The voltage was swept at a scan rate of 1.0 mV s$^{-1}$. Electrochemical measurements of the hybrid ionogel polymer electrolytes were conducted using 2032 coin cells consisting of a separator, Li metal and $LiFePO_4$ (90 wt% $LiFePO_4$, 5 wt% carbon black, and 5 wt% PVDF) electrodes. All the cells were assembled in argon-charged glove box. After fabrication, the cells with pre-gel solution was subjected to thermal cross-linking for 3 h at 70 °C. The galvanostatic charge-discharge experiments were carried out with voltage range of 2.2–3.8 V using a battery cycler (Wonatech, WBCS3000) at room temperature.

## Results and Discussion

### Synthesis of LPEOMASQ Copolymers and Fabrication of PEGylated Hybrid Ionogels

PEO-functionalized ladder-structured polysilsesquioxanes were synthesized using our previous method,[24, 25] a base-catalyzed aqueous sol-gel reaction, in which various comonomer compositions, 25:75, 50:50, 75:25, of 2-[methoxy(polyethyleneoxy)propyl]trimethoxysilane and 3-methacryloxypropyltrimethoxysilane were hydrolyzed and condensed *in-situ*. (Scheme 1a) Obtained hybrid polymers were named as such: LPEOMASQ25, LPEOMASQ50, LPEOMASQ75 according the PEO comonomer percentage. Through design of the comonomers, crosslinkable ladder-structured polysilsesquioxanes with free-dangling PEO groups were introduced at the molecular level. These LPEOMASQ compounds then were utilized to crosslink ionic liquid solutions of 1M LiTFSI in BMPTFSI at a low concentration of 5 wt %.

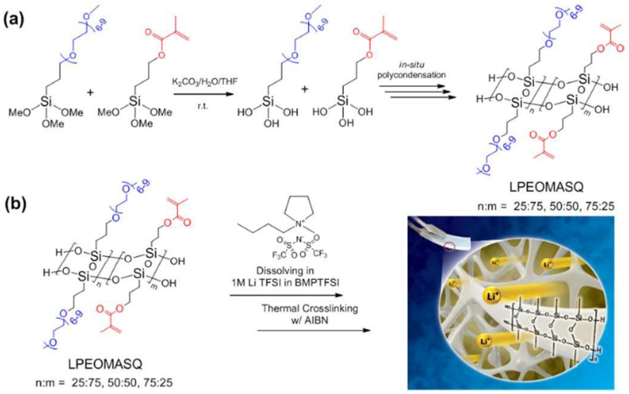

**Scheme 1.** (a) Synthesis of LPEOMASQ series and (b) fabrication of PEGylated Hybrid Ionogels

The characterization of the LPEOMASQ compounds were conducted with $^1$H NMR, $^{29}$Si NMR, and FTIR, as shown in Fig. 1. $^1$H NMR of the LPEOMASQ compounds showed that the methacryloxypropyl groups and PEG groups were introduced according to their initial comonomer ratio as indicated by the increasing large signal at 3.7 ppm, attributed to the ethylene oxide proton, as the PEG-ratio increased from LPEOMASQ25 to LPEOMASQ75. Moreover, no discernible peaks were found at 5.0 ppm, attributed to the uncondensed silanol Si-OH end groups.[26] Also, $^{29}$Si NMR results revealed the presence of two large signals centered at -67 and -69 ppm, attributed to the fully condensed $T^3$ Si-O-Si structure of Si-methacryloxypropyl-(Si-MMA) and 2-[methoxy(polyethyleneoxy)propyl (Si-$C_3$-PEG) groups, respectively.[27] As shown, the relative intensity of the $T^3$ for Si-$C_3$-PEG at -69 ppm (assigned as *X*) increased as the PEG-ratio increased from LPEOMASQ25 to LPEOMASQ75, and the relative integrative ratio between the $T^3$ for Si-$C_3$-PEG at -69 ppm (assigned as *X*) and $T^3$ for Si-methacryloxypropyl at -67 ppm (assigned as *Y*) reflected the initial comonomer feed ratio. Also noteworthy is the lack of signals near -58 ppm, which are the charcateristics chemical shifts for the uncondensed $T^2$ alkyl-silicons, as this provides additional evidence for the fully condensed, ladder-like structure of the LPEOMASQ compounds. FTIR spectra revealed the presence of C=O, and C=C, and Si-O-Si bands centered at 1745 cm$^{-1}$, 1638 cm$^{-1}$, and 1050 cm$^{-1}$, 1100 cm$^{-1}$, respectively.

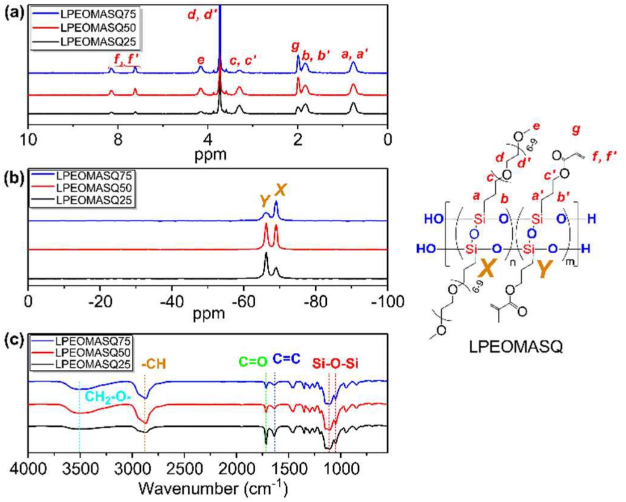

**Fig 1.** (a) $^1$H NMR, (b) $^{29}$Si NMR, and (c) FTIR spectra for the PEGylated LPSQs

The hybrid ionogels were prepared via a thermally curing process. The unsaturated vinyl groups of the methacryloxypropyl- moieties in ladder-like poly(methacryloxypropyl-co-polyethyleneoxide)silsesquioxane (LPEOMASQ) were cross-linked in an ionic liquid solution of 1 M LiTFSI in BMPTFSI to form a polymeric network structure, resulting in an mechanically stable and homogeneous ionogels as shown in Fig 2. As shown, the disappearance of peaks assigned to the C=C bonds at 1638 cm$^{-1}$ was determined by FT-IR after thermal treatment. To eliminate mitigating factors of crosslinker concentration, we fabricated the PEGlyated hybrid ionogels with equal concentrations (5 wt%) of LPEOMASQs. Furthermore, the dynamic viscoelastic properties of the thermally cured hybrid ionogels as a function of frequency are presented in Fig. 2b. For all ionogel samples, the response of dynamic modulus was seen to be nearly independent of the applied frequency and the elastic modulus G' was greater than storage modulus G'', indicating predominantly solid-like viscoelastic behavior.[34-36] Moreover, the effect of increasing PEO content was to plasticize the hybrid ionogel, as LPEOMASQ75 5 wt% exhibited the lowest modulus and LPMASQ 5 wt%, which has no PEO groups, giving the highest modulus values across all frequencies. This was in due part to the free-dangling oligomeric PEO groups, which at room temperature existed in the melt-phase given the liquid state of of the neat PEGylated LPSQs. Moreover, given that all of the LPEOMASQ gels exhibited solid-like behaviour, even the low MMA content of LPEOMASQ25 contained enough crosslinking functionality for obtaining mechanically robust hybrid gels.

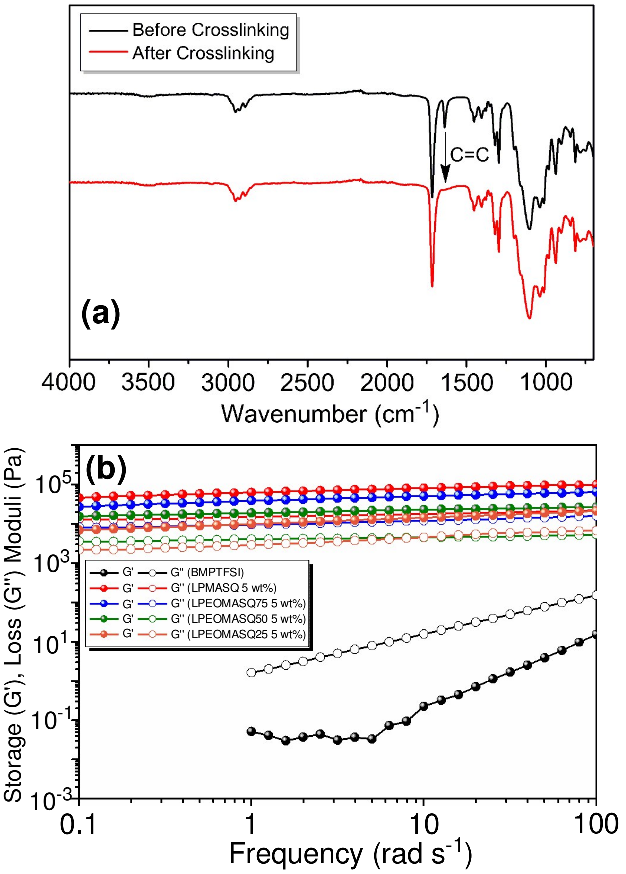

**Fig 2.** (a) FTIR spectra of LPEOMASQ75 5 wt% before and after crosslinking and (b) rheological properties of the IL and hybrid ionogels

### Ion Conduction in PEGylated Hybrid Ionogels

Fig. 3a compares the measured ionic conductivities as a function of temperature. As presented, gelation of ionic liquids provided an undeniable depreciating effect on ionic conductivity, while enabling mechanical support and dimensional stabilization. Such decreased ionic conductivity ($\sigma$) of the electrolyte can be described using the following equation.

$$\sigma (T) = \Sigma\, n \times q \times \mu$$

where $n$ is the number of charge carriers, q is the charge on the charge carrier, and $\mu$ is the mobility of charge carriers.[28] The decrease in ionic mobility and the number of ions per unit volume of electrolyte, caused by the introduction of the crosslinking agent, is attributed to the deteriorated ionic conductivity. Interestingly, the incorporation of ethylene oxide groups into network structure led to the increase in ionic conductivity. Moreover, we observed the ionic conductivity increased continuously with increasing the content of ethylene oxide groups. It should be note that the amount of crosslinker contents was the same in ionogel systems, held constant at 5 wt%. Considering the number of charge carrier was invariant, the observed ion transport behavior could be explained by the change in mobility of charged species. We speculated that the efficient diffusion of ions in PEGylated network structure correlated with the ability of ion dissociation and conduction that facilitates ion transport.[29, 30]

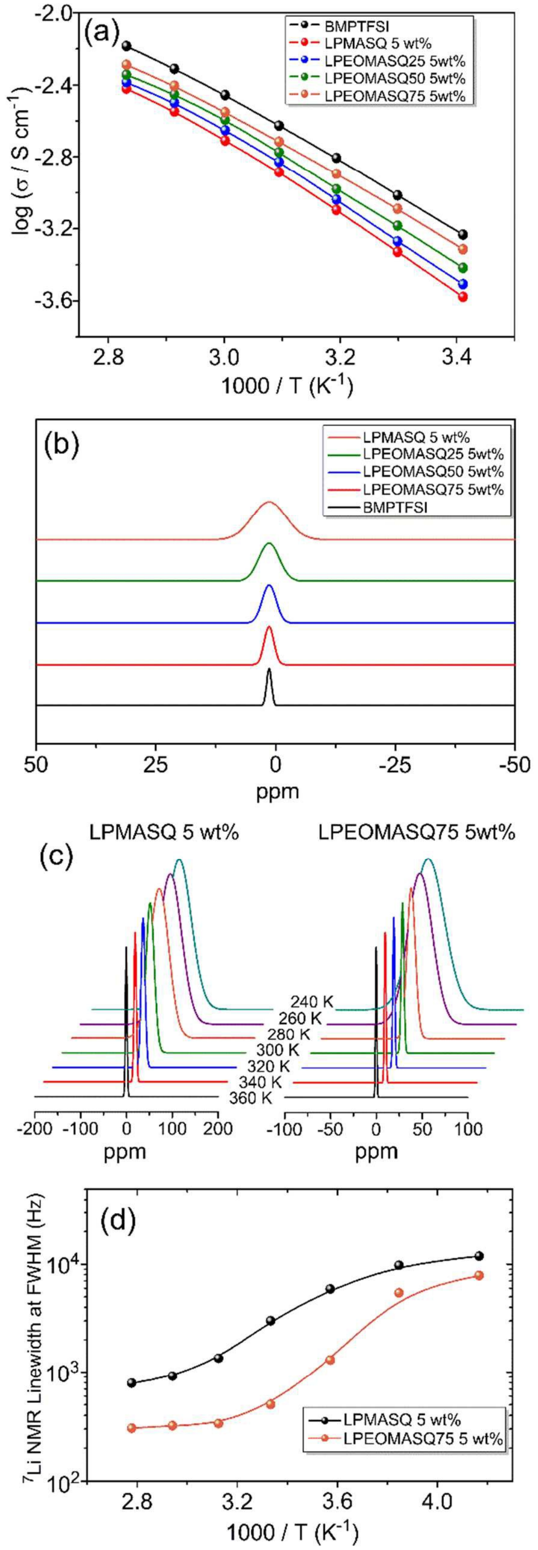

**Fig. 3** (a) Temperature dependent ionic conductivities, (b) Solid-state 7Li NMR spectra for the IL and hybrid ionogels, (c) temperature-dependent Solid-state 7Li NMR spectra of LPMASQ 5 wt% and LPEOMASQ75 5 wt%, and (d) 7Li NMR linewidth summary

As such, we conducted solid-state $^7$Li NMR single-pulse experiments comparing the neat ionic liquid and the various hybrid ionogels as shown in Fig. 3b, to probe the ability of ion dissociation and conduction of lithium ions. As shown, while the neat IL showed a very sharp peak attributed to the lithium cation derived from the lithium salt dissolved in IL, the $^7$Li NMR linewidth for the hybrid ionogels revealed a noticeable degree of decrease, or sharpening effect, as the PEO comonomer content increased from LPMASQ (0%) (chemical structure shown in ESI, Fig. S1) to LPEOMASQ13 (75%). This point was further explored by the temperature dependent solid state $^7$Li NMR spectra comparing LPMASQ and LPEOMASQ75 (Fig. 2c), which showed the rapid sharpening of the $Li^+$ peak starting around 35 °C (Fig. 3d), correlating to the melt-phase state of the ionic liquid confined in the hybrid matrix.[9] It was clear from these NMR results that the effect of free-dangling PEGs on the lithium salt was pronounced in effectively dissociating the TFSI anion from lithium cation. This was a noteworthy result, as the effect was only previously demonstrated with zwitterionic compounds and single-ion conducting compounds, which functioned to immobilize the anion completely.[31] Further distinguishing from these previously results, is the low concentration of crosslinker (5 wt%) required to fully gel the liquid solution, due to the hybrid inorganic backbone delivering mechanical robustness further showcasing the inherent high and effective ion conduction behavior of these hybrid PEGylated ionogels for practical commercial performance.

Moreover, solid-state $^{19}$F NMR single-pulse experiments with the PEGylated hybrid ionogels (Fig. 4a) showed similar peak sharpening effect as the fluorines derived from the TFSI anions were more dissociated for those hybrid gels containing greater concentration of PEO groups. To better understand the observed intermolecular interaction, we characterized the extent of ion pair formation using Raman analysis. It has previously reported that the strong Raman bands at 742 cm$^{-1}$ and 748 cm$^{-1}$ correspond to the free, or dissociated TFSI$^-$ ions and the bonded, or associated $Li^+$ TFSI$^-$ ion pairs, respectively.[32, 33] As shown Fig. 4b, we observed changes in $Li^+$ coordination with PEO concentration that may possibly contribute to an increase in ionic mobility. It can be clearly seen that there was a weak interaction in LPEOMASQ ionogels over the non-PEO containing LPMSASQ ionogel counterpart. When considering the minimal contribution of the highly sterically hindered ester groups of the crosslinked MMA junctions to ionic conductivity in our hybrid ionogels, and that the PEO-groups are only functionalized to the silicon backbone on one end, or free-dangling, we attributed the increase in ionic mobility and ionic conductivity to the melt-phase, liquid-like, free-dangling PEO groups.

Before evaluating the electrochemical performances of the ionogels, we assessed the electrochemical stability using linear sweep voltammometry (LSV) measurements. As shown in ESI Fig. S2, no abrupt rise in oxidative current related to the electrochemical decomposition of the electrolyte was detected below 5.0 V in the anodic sweep, demonstrating that the prepared ionogels were electrochemically stable up to 5.0 V, which could be utilized in high-voltage lithium batteries. Additionally, the thermal stability of ionogels was investigated. As depicted in ESI Fig. S3, these ionogels exhibited excellent thermal stability with no obvious weight loss observed at temperatures exceeding 350 °C. Moreover, this high thermal stability of indistinguishable decomposition of residual silanol groups, thus full condensation of the Si-O-Si backbone, rendered the high electrochemical stability of the PEGylated hybrid ionogels.

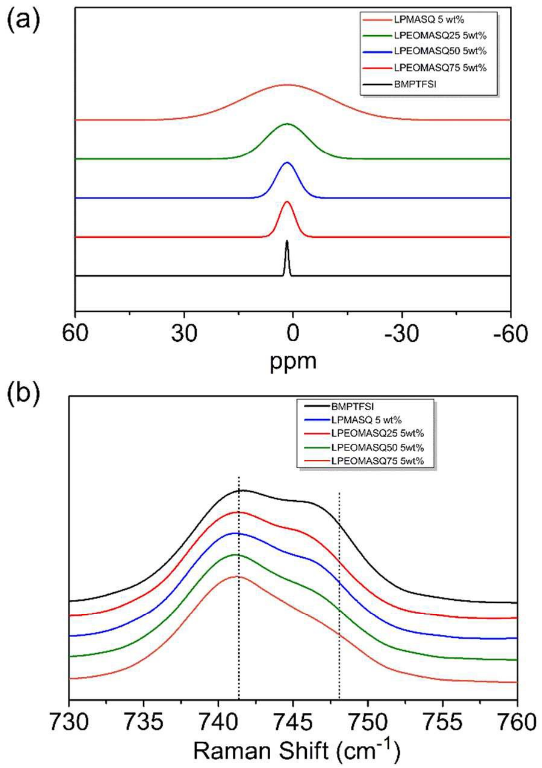

**Fig 4.** (a) Solid-state $^{19}$F NMR spectra at room temperature and (b) Raman spectra

### Electrochemical Cell Performance

We fabricated $LiFePO_4$/lithium cells assembled with hybrid ionogels (95 wt % of ionic liquid containing 5 wt% cross-linker) to characterize the electrochemical performance of the hybrid PEGylated ionogels. Fig. 5a presents the rate capabilities of the cells with different cross-linker systems. For the test, the cells were charged at a constant current density of 0.1 C (1 C rate corresponded to a current density of 155.1 mA g $^{-1}$) and discharged at various current densities in a voltage range of 2.5-4.2 V. At a low current rate of 0. 1 C, the reversible discharge capacity of LPEOMASQ hybrid ionogels was 148.9 mAh g$^{-1}$, which was slightly larger than that of cells containing ionogels without PEO groups, LPMASQ. However, upon the increase in the current rate, the LPEOMASQ PEGylated hybrid ionogels cells exhibited improved capacity retention. For instance, the cell fabricated with LPEOMASQ ionogel retained 47.2 % of its initial capacity, whereas the cell containing LPMASQ ionogel retained 33.1 % at a current rate of 0.5 C. In general, rate capability of cell suffered from poor kinetics at the electrode-electrolyte interface.[37] As expected, the capacity degradation was closely coupled with ion transport of different electrolyte systems. Thorough these results, we stipulated that the enhanced electrochemical performance achieved in this work was due in part to the incorporation of free-dangling PEO groups in the network structure, promoting transport of lithium ions' heightened ability to dissociate from the anion, thereby alleviating the ohmic polarization loss of the cell.[38]

The cycling performance of the cells was evaluated further through measuring the discharge capacities, where the cells were charged at a current density of 0.1 C and discharged 0.1 C. Fig. 5b presents the charge/discharge capacity and Columbic efficiency as a function of cycle number. As shown, the cycling behaviors of the cells containing LPEOMASQ hybrid ionogels were more stable in the following cycles. In the initial stages of cycling, reversible discharge capacities reached 148.2 mAh $g^{-1}$, which was close to the cells fabricated with the liquid 1 M LiTFSI BMPTFSI (ESI, Fig. S4). The retained discharge capacity was 136.6 mAh $g^{-1}$ after 50 cycles and the Columbic efficiency of the system was observed to be nearly 99 %. In addition, as depicted in Fig. 5b inset, a well-defined voltage plateau around 3.4 V (vs. $Li/Li^+$) associated to the lithium insertion/extraction into cathode materials was a highly maintained and repeatable process,[39] confirming the sufficient mobility of lithium ions and electrochemical stability of these PEGylated hybrid ionogels. Therefore, we clearly demonstrated that the incorporation of polyethyleneoxide groups in the network structure could help facile ion transport of hybrid ionogels, resulting in improved electrochemical performance.

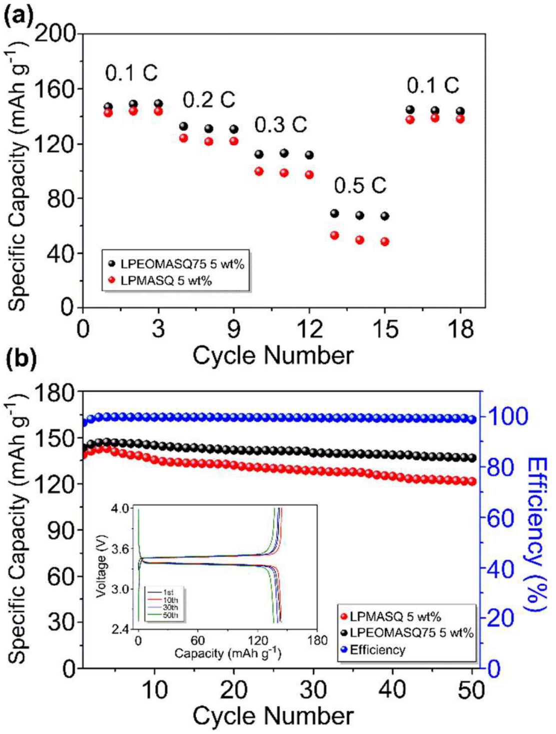

**Fig 5.** (a) Discharge capacities at various C-rates for $LiFePO_4$/Hybrid Ionogel/Li cells and (b) Cyclabilty of PEGylated hybrid ionogels with inset showing the charge-discharge profiles at selected cycle number

## Conclusions

In conclusion, we synthesized a series of PEGylated ladder-structured polysilsesquioxanes with various PEG:methacryloxypropyl copolymer ratios. Chemical crosslinking of the methacryl groups in a 1M LiTFSI N-butyl-N-methylpyrrolidinium bis(trifluoromethylsulfonyl)imide ionic liquid solution at a low concentration of 5 wt% yielded PEGylated hybrid ionogels. Through an in-depth spectroscopic investigation of the ion conduction behavior of these PEGylated hybrid ionogels and comparison with hybrid ionogels without PEG groups, we were able to demonstrate how enhancement in lithium ion battery performance for PEGylated hybrid iongels could be achieved at identical crosslinker concentrations.

## Acknowledgements

This work was financially supported by a grant from the Fundamental R&D Program for Core Technology of Materials and the Industrial Strategic Technology Development Program funded by the Ministry of Knowledge Economy, Republic of Korea, and partially by a grant from Materials Architecturing Research Centre of the Korea Institute of Science and Technology (KIST).

## Notes and references

1 J. M. Tarascon and M. Armand, *Nature*, 2001, **414**, 359-367.
2 N.-S. Choi, Z. Chen, S. A. Freunberger, X. Ji, Y.-K. Sun, K. Amine, G. Yushin, L. F. Nazar, J. Cho and P. G. Bruce, *Angew. Chem. Int. Ed.*, 2012, **51**, 9994-10024.
3 E. Quartarone and P. Mustarelli, *Chem. Soc. Rev.*, 2011, **40**, 2525-2540.
4 Y. Wang and W.-H. Zhong, *ChemElectroChem*, 2015, **2**, 22-36.
5 K. Xu, *Chem. Rev.*, 2004, **104**, 4303-4418.
6 Z. Chen, Y. Ren, A. N. Jansen, C.-k. Lin, W. Weng and K. Amine, *Nat. Commun.*, 2013, **4**, 1513.
7 J. Le Bideau, L. Viau and A. Vioux, *Chem. Soc. Rev.*, 2011, **40**, 907-925.
8 S. A. M. Noor, P. M. Bayley, M. Forsyth and D. R. MacFarlane, *Electrochim. Acta*, 2013, **91**, 219-226.
9 M. P. Singh, R. K. Singh and S. Chandra, *Prog. in Mater. Sci.*, 2014, **64**, 73-120.
10 J. H. Lee, A. S. Lee, J.-C. Lee, S. M. Hong, S. S. Hwang and C. M. Koo, *J. Mater. Chem. A*, 2015, **3**, 2226-2233.
11 Y. Lu, K. Korf, Y. Kambe, Z. Tu and L. A. Archer, *Angew. Chem. Int. Ed.*, 2014, **53**, 488-492.
12 Y. Lu, S. S. Moganty, J. L. Schaefer and L. A. Archer, *J. Mater. Chem.*, 2012, **22**, 4066-4072.
13 J.-A. Choi, Y. Kang and D.-W. Kim, *Electrochim. Acta*, 2013, **89**, 359-364.
14 C. Liao, X.-G. Sun and S. Dai, *Electrochim. Acta*, 2013, **87**, 889-894.
15 M. Popall, M. Andrei, J. Kappel, J. Kron, K. Olma and B. Olsowski, *Electrochim. Acta*, 1998, **43**, 1155-1161.
16 A. I. Horowitz and M. J. Panzer, *J. Mater. Chem.*, 2012, **22**, 16534-16539.
17 L. Viau, M.-A. Néouze, C. Biolley, S. Volland, D. Brevet, P. Gaveau, P. Dieudonné, A. Galarneau and A. Vioux, *Chem. Mater.*, 2012, **24**, 3128-3134.
18 F. Gayet, L. Viau, F. Leroux, S. Monge, J.-J. Robin and A. Vioux, *J. Mater. Chem.*, 2010, **20**, 9456-9462.

*19* K. Ueno, K. Hata, T. Katakabe, M. Kondoh and M. Watanabe, *J. Phys. Chem. B.*, 2008, **112**, 9013-9019.
20 J. L. Schaefer, D. A. Yanga and L. A. Archer, *Chem. Mater.*, 2013, **25**, 834-839.
21 S. S. Moganty, S. Srivastava, Y. Lu, J. L. Schaefer, S. A. Rizvi and L. A. Archer, *Chem. Mater.*, 2012, **24**, 1386-1392.
22 M.-A. Néouze, J. L. Bideau, P. Gaveau, S. Bellayer and A. Vioux, *Chem. Mater.*, 2006, **18**, 3931-3936.
23 A. S. Soo Lee, J. H. Lee, J.-C. Lee, S. M. Hong, S. S. Hwang and C. M. Koo, *J. Mater. Chem, A*, 2014, **2**, 1277-1283.
24 A. S. Lee, Y. Y. Jo, H. Jeon, S.-S. Choi, K.-Y. Baek and S. S. Hwang, *Polymer*, 2015, **68**, 140-146.
25 A. S. Lee, S. S. Choi, S. J. Song, K. Y. Baek and S. S. Hwang, *RSC Adv.*, 2014, **4**, 56532-56538.
26 S.-S. Choi, A.S. Lee, S.S. Hwang and K.-Y. Baek, *Macromolecules*, 2015, **48**, 6063-6070.
27 S. S. Choi, A. S. Lee, H. S. Lee, H. Y. Jeon, K. Y. Baek, D. H. Choi and S. S. Hwang, *J. Polym Sci. Part A: Polym. Chem.*, 2011, **49**, 5012-5018.
28 S.-J. Kwon, D.-G. Kim, J. Shim, J. H. Lee, J.-H. Baik and J.-C. Lee, *Polymer*, 2014, **55**, 2799-2808.
29 D. Zhou, Y.-B. He, R. Liu, M. Liu, H. Du, B. Li, Q. Cai, Q.-H. Yang and F. Kang, *Adv. Energy Mater.*, 2015, **5**.
30 F. Croce, M. L. Focarete, J. Hassoun, I. Meschini and B. Scrosati, *Energy Environ. Sci.*, 2011, **4**, 921-927.
31 C. Tiyapiboonchaiya, J. M. Pringle, J. Sun, N. Byrne, P. C. Howlett, D. R. MacFarlane and M. Forsyth, *Nat. Mater.*, 2004, **3**, 29-32.
32 M. J. Monteiro, F. F. C. Bazito, L. J. A. Siqueira, M. C. C. Ribeiro and R. M. Torresi, *J. Phys. Chem. B*, 2008, **112**, 2102-2109.
33 L. J. Hardwick, M. Holzapfel, A. Wokaun and P. Novák, *J. Raman Spectrosc.*, 2007, **38**, 110-112.
34 M. Yoshida, N. Koumura, Y. Misawa, N. Tamaoki, H. Matsumoto, H. Kawanami, S. Kazaoui and N. Minami, *J. Am. Chem. Soc.*, 2007, **129**, 11039-11041.
35 M. Patel and A. J. Bhattacharyya, *Energy Environ. Sci.*, 2011, **4**, 429-432.
36 M. Patel, M. Gnanavel and A. J. Bhattacharyya, *J. Mater. Chem.*, 2011, **21**, 17419-17424.
37 M. Wetjen, M. A. Navarra, S. Panero, S. Passerini, B. Scrosati and J. Hassoun, *ChemSusChem*, 2013, **6**, 1037-1043.
38 S.-H. Kim, K.-H. Choi, S.-J. Cho, E.-H. Kil and S.-Y. Lee, *J. Mater. Chem. A*, 2013, **1**, 4949-4955.
39 L.-X. Yuan, Z.-H. Wang, W.-X. Zhang, X.-L. Hu, J.-T. Chen, Y.-H. Huang and J. B. Goodenough, *Energy Environ. Sci.*, 2011, **4**, 269-284.